MINISTÉRIO DA EDUCAÇÃO
UNIVERSIDADE FEDERAL DO RIO GRANDE DO SUL
PROGRAMA DE PÓS-GRADUAÇÃO EM ENGENHARIA MECÂNICA

NUMERICAL STUDY OF RADIATIVE HEAT LOSS ON NEAR-EXTINCTION LAMINAR NON-PREMIXED FLAMES EMPLOYING DETAILED CHEMISTRY AND THE FGM METHOD

por

Fredherico Nicolaus Rodrigues da Silva

Dissertação para obtenção do Título de
Mestre em Engenharia

Porto Alegre, Julho de 2020

NUMERICAL STUDY OF RADIATIVE HEAT LOSS ON NEAR-EXTINCTION LAMINAR NON-PREMIXED FLAMES EMPLOYING DETAILED CHEMISTRY AND THE FGM METHOD

por

Fredherico Nicolaus Rodrigues da Silva
Engenheiro Mecânico

Dissertação submetida ao Corpo Docente do Programa de Pós-Graduação em Engenharia Mecânica, PROMEC, da Escola de Engenharia da Universidade Federal do Rio Grande do Sul, como parte dos requisitos necessários para a obtenção do Título de

Mestre em Engenharia

Área de Concentração: Fenômenos de Transporte

Orientador: Fernando Marcelo Pereira

Aprovada por:

Prof. Dr. Felipe Crivellaro Minuzzi .....Escola Politécnica / Unisinos

Prof. Dr. Felipe Roman Centeno ..... PROMEC / UFRGS

Prof. Dr. Thiago Cardoso de Souza .....PPGEM / UFRN

Prof. Dr. Jakson Manfredini Vassoler
Coordenador do PROMEC

Porto Alegre, 24 de Julho de 2020

À minha avó, Lorena.

There is no knowledge that's not power

Unkown

AGRADECIMENTOS

À Carolina, que esteve do meu lado durante todo esse caminho, especialmente nas horas mais difíceis, apoio sem o qual não teria chegado até aqui.

À minha família que sempre me apoiou durante toda minha vida.

Ao meu orientador, Professor Fernando Pereira, por todo apoio que me dedicou durante os últimos anos, bem como os outros Professores do Promec, em especial ao Professor Francis França e o Professor Paulo Schneider.

À banca examinadora, que teve a disposição e dedicação para avaliar este trabalho, contribuindo para o seu aperfeiçoamento e minha formação.

Aos meus colegas de Universidade e especialmente do Laboratório de Combustão, que sempre ajudaram a manter a moral elevada, e em especial aos que ao longo do tmepo se envolveram diretamente e contribuíram para esse trabalho, como o Cristian Hoerlle, André Contini, Renan Kops e Leonardo Donatti.

Aos amigos de longa data que se mantiveram ao meu lado, em especial o Jean, o Ferri, Larissa, Pedro, David, e inúmeros colegas de curso os quais seria impossível citar todos.

Ao Conselho Nacional de Desenvolvimento Científico e Tecnológico (CNPq) pelo suporte financeiro para a elaboração deste trabalho.

RESUMO

Esta dissertação tem como objetivo o estudo de differentes abordagens para a solução do problema radiante em chamas difusivas laminares. Ao longo deste trabalho, o código Chem1d é usado extensivamente para o estudo de estruturas unidimensionais conhecidas como flamelets, as quais representam as equações de transporte, cinética química e transferência de calor de uma chama, desacopladas das equações de escoamento. Essa abordagem torna possível a solução de chamas com cinética química detalhada acoplado ao problema radiativo em baixos tempos computacionais, ordens de grandeza mais rápidos que as atuais simulações multidimensionais. O código conta com o modelo de gás cinza para o limite opticamente fino (Optically Thin Approximation - OTA). Além deste, o modelo de soma ponderada de gases cinzas (WSGG), bem como o método de integração Linha-por-Linha (LBL) foram implementados, e comparações entre as três abordagens são efetuadas. Para melhor estudar os efeitos da radiação, as simulações empregam diluições de N_2 e CO_2 ao combustível. A validação das presentes soluções se dá pela comparação de perfis de velocidade e temperatura com soluções disponíveis na literatura, bem como a comparação dos termos fontes radiantes. Em seguida, os limites de extinção são investigados, aumentando-se a diluição para os modelos OTA e WSGG a diferentes taxas de deformação. Os resultados são comparados a dados numéricos e experimentais disponíveis na literatura, mostrando que existe uma taxa de deformação limite abaixo da qual as soluções unidimensionais não conseguem corretamente reproduzir os perfis experimentais devido a perdas de calor laterais e, no caso de chamas a gravidade terrestre, presença de empuxo. Posteriormente o estudo da perda de calor radiante para chamas não pré-misturadas é investigado na técnica Flamelet Generated Manifold (FGM). Um manifold tridimensional é construído empregando o enthalpy defect como uma nova variável para mapear a perda de calor. O processo para a obtenção e geração dos conjuntos de flamelets necessários para a construção do manifold é detalhadamente explicado e um manifold empregando flamelets estáveis é utilizado para investigar chamas não-adiabáticas, comparando soluções OTA, WSGG e LBL às suas respectivas contrapartes detalhadas. As soluções FGM se mostraram satisfatoriamente semelhantes aos perfis detalhados, com grande redução no tempo computacional. Posteriormente, um manifold utilizando flamelets instáveis foi construído para investigar os limites de extinção com os modelos OTA e WSGG, mostrando

mais uma vez que as soluções FGM se aproximam satisfatoriamente dos resultados de química detalhada.

Palavras-chave: Chama não pré-misturada; Modelos de radiação; Chama unidimensional; Cinética química detalhada; Flamelet generated manifold (FGM); Enthalpy defect.

ABSTRACT

This thesis aims to explore different approaches for the solution of the radiative problem on laminar diffusion flames. Throughout this work, the Chem1d code is extensively used for the study of one-dimensional flame structures known as flamelets, which represents the transport, chemical kinetics and radiative heat transfer equations decoupled from flow equations. This approach makes possible the solution of detailed chemistry flames coupled with the radiative problem in low computational times, orders of magnitude faster than the current multidimensional flame simulations. Chem1d counts with a thin optic limit grey-gas model (Optically Thin Approximation - OTA). Additionaly, the Weighted Sum of Grey-Gases model (WSGG), as well as the Line-by-Line integration method (LBL) were implemented to the code, with comparisons for the three approaches taking place. For a better visualization of the radiation effects, simulations employ dilutions with N_2 and CO_2 for the fuel side. Validation of the present solutions is given by a comparison of velocity and temperature profiles with literature data, as well as comparisons of the radiative heat source. Following this, the extinction limits for the OTA and WSGG models are investigated, with dilutions being increased up until flame extinction for different strain rates. Results are compared to numerical and experimental literature data, showing that there exists a limit strain rate for which lower values cannot correctly reproduce experimental profiles, due to lateral heat losses and, for Earth's gravity conditions, the presence of buoyancy. Later, the study of radiative heat loss for non-premixed flames is investigated in the Flamelet Generated Manifold (FGM) technique. A three dimensional manifold is constructed employing the enthalpy defect as a new control variable to map heat loss. The process for the generation of sets of flamelets with the required enthalpy defect levels is described and a manifold with the use of stable flamelet solutions is constructed and used to investigate non-adiabatic flames, comparing OTA, WSGG and LBL solutions to each respective detailed chemistry counterpart. FGM solutions show to be satisfactorily similar to the detailed profiles, with a great reduction in computational time. Lastly, a manifold employing the unsteady flamelet solutions is constructed to study extinction limits within the FGM method with the OTA and WSGG models, showing once more that the FGM solutions adequately approach the detailed chemistry results.

Keywords: Non-premixed flame; Radiation models; One-dimensional flame; Detailed chemical kinetics; Flamelet generated manifold (FGM); Enthalpy defect.

Contents

LIST OF FIGURES

LIST OF TABLES

LIST OF ABBREVIATIONS

CFD	Computational Fluid Dynamics
CHEM1D	One-dimensional laminar flame code
DOM	Discrete Ordinate Method
FGM	Flamelet-Generated Manifold
LBL	Line-by-Line
L.H.S.	Left Handed Side
OTA	Optically Thin Approximation
PROMEC	Programa de Pós-Graduação em Engenharia Mecânica
R.H.S.	Right Handed Side
UFRGS	Universidade Federal do Rio Grande do Sul
WSGG	Weighted Sum of Grey-Gases

LIST OF SYMBOLS

Latin Symbols

a	Strain rate, s^{-1}
a_g	Global strain rate, s^{-1}
a_l	Local strain rate, s^{-1}
a_i	Temperature dependent weighting coefficient, $-$
A_r	Pre-exponential factor, $-$
$b_{i,j}$	Polynomial coefficient of order j for the gas i
c_p	Specific heat constant at constant pressure of the mixture, $J/(kg\,K)$
$c_{p,i}$	Specific heat constant at constant pressure of species i, $J/(kg\,K)$
C_i	Concentration of species i, $-$
$D_{i,j}$	Binary diffusion coefficient of species i into species j, m^2/s
D_i^M	Mixture average diffusion coefficient, m^2/s
E_a	Activation energy, J/mol
$\vec{g}$	Gravity acceleration vector, m/s^2
h	Enthalpy of mixture, J/kg
h_i	Enthalpy of species i, J/kg
$h_{i,f}^0$	Enthalpy of formation of species i, J/kg
I	Identity tensor, $-$
I_η	Radiative intensity, W/m^2
$I_{\eta,b}$	Black body radiative intensity, W/m^2
k_f	Forward reaction constant, $-$
k_r	Reverse reaction constant, $-$
k_p	Mean Planck absorption constant, m^{-1}
$k_{p,i}$	Mean Planck absorption constant for species i, m^{-1}
K	Strain rate, s^{-1}
Le_i	Lewis number, $-$
m_i	Mass of species i, kg
MW_i	Molecular weight of species i, g/mol
N_{gg}	Number of grey gases, $-$
p	Mixture pressure, N/m^2

p_i	Partial pressure of species i, N/m^2
p_0	Atmospheric pressure, N/m^2
$\vec{q}$	Heat flux, W/m^2
$\dot{q}_R$	Radiative heat source, W/m^3
$\dot{Q}$	Integrated radiative heat source, W/m^2
R_u	Universal gas constant, $J/(mol\ K)$
S	Spatial direction, $-$
$\dot{S}$	Integrated heat release rate, W/m^2
t	Time, s
T	Temperature, K
T_{ref}	Reference temperature, K
$\vec{u}$	Flow velocity vector, m/s
v_i	Number of moles of species i
$\vec{V_i}$	Molecular diffusion velocity vector of species i, m/s
X_i	Molar fraction of species i, $-$
X_r	Radiative fraction, $-$
Y_i	Mass fraction of species i, $-$
Z	Mixture fraction, $-$

Greek Symbols

α	Thermal diffusivity, m^2/s
α_i	Weight factor of species i, mol/g
β_r	Temperature exponent, $-$
η	Wave number, m^{-1}
λ	Thermal conductivity coefficient, $W/(m\ K)$
κ_η	Spectral absorption coefficient, m^{-1}
$\kappa_{\eta,p}$	Pressure dependent spectral absorption coefficient, m^{-1}
ρ	Mixture density, g/m^3
$\phi_{i,j}$	Control variable, $-$
$\Phi_{i,j}$	Dimensionless quantity, $-$
$\dot{\omega}_i$	Reaction source term of species i, $g/(m^3 s)$
ω_j	Molar reaction rate of species j, $mol/(m^3 s)$
Ω_l	Solid angle, sr

μ_i	Dynamic viscosity, $kg/(ms)$
τ	Stress tensor, N/m^2
σ	Stefan-Boltzmann constant, $W/(m^2K^4)$
$\mathcal{Y}$	Progress Variable, $-$
ζ	Enthalpy defect, kJ/kg

1 INTRODUCTION

The use of fire has been an intrinsic part of the human existence for millions of years. Fire is essential to our daily lives, with combustion processes taking up to 90% of the current world primary energy supply in 2019 [IEA, 2019], and projections for the use of natural gas burners growing over 33% by 2050 in the United States alone [EIA, 2020]. A major portion of this energy is provenient from non-premixed, or diffusion, flames, a type of flame where fuel and oxidant combine and react through molecular diffusion of the chemical species. Diffusion flames are present from household candles and ovens to industrial gas burners and flares. They tend to be highly luminous compared to premixed flames, which results in a high thermal radiation emission.

Thermal radiation is an important heat transfer process for non-premixed flames. It has been the subject of extensive studies, with its understanding being critical for the energy generation industry. Numerically, the problem lies on the determination of the local radiative heat source, which demands accurate prediction of participating gases and flame temperature, and although radiation in combustion processes have been extensively studied recently, these models are usually developed and validated by solving idealized one-dimensional problems with imposed temperature and species distributions or with the use of global chemical mechanisms. The coupling of the detailed chemistry, transport equations, flow equations and radiative heat losses is highly computationally demanding, with new approaches for faster and more efficient solutions constantly being researched.

One-dimensional flames have been studied since the beginning of combustion science due to their simplicity and, mainly, because they can closely represent a number of characteristics of real flames. For example, the concept of the burning velocity of premixed flames is a well-defined fundamental property of a fuel/oxidant mixture only for a hypothetical one-dimensional flame. In diffusion flames, the canonical configuration is the counterflow flame, which can be approximately modeled by 1D conservation equations subjected to stretch effects, by the outer flow field, to take into account deviations from the one-dimensional approximation imposed. Even multidimensional turbulent flames are seen as an ensemble of one-dimensional flames (flamelets). Many numerical schemes rely on this concept. The idea being that one-dimensional flame structures can be used to study detailed chemistry and transport equations decoupled from multidimensional flow,

resulting in highly accurate solutions for low computational times. The advantage of this procedure is the possibility of producing different conditions that are relevant for actual flames. Flamelets are usually very thin, with a size of a few milimeters in length and small optical thicknesses Thus, radiation heat losses, although relevant for capturing details of the flame structure, can be neglected as a first approximation.

In some combustion problems however, the optical thickness may be small while the radiative heat loss still plays a central role. This is the case for some flames near the extinction limit, for example, a situation in which an increase or decrease of heat losses by a small amount may define the existence or not of a stable flame. Thus, the study of near-extinguished flames is an area of great interest for the research and improvement of thermal radiation models. To achieve such critical flame conditions, the addition of dilutants such as N_2 or CO_2 in the fuel stream is commonly used. As the concentration of fuel in the mixture becomes critical, any heat losses due to radiation will cause flame extinction.

The present study will explore the laminar counterflow flame configuration, where opposing streams of fuel and oxidant react near the stagnation plane. The higher the velocity of the reactant streams, the higher the strain on the flame and the more stretched the flame appears. For relatively low stretched flames, flame extinction is governed by radiation, as residence times approaches those of equilibrium flames. As strain rate increases, the role of radiative heat loss decreases and residence time effects start to dominate. It can be seen thus that the structure of the flame is determined by a balance of radiation and strain effects.

On the other hand, the solution of detailed chemistry is another highly demanding process. The combustion of CH_4 for example can be modeled with highly optimized mechanisms such as GRI Mech [Smith et al., 2000], with its most recent version accounting for 325 reactions and 55 chemical species. Reduced mechanisms such as DRM 19 [Kazakov and Frenklach, 2005] are an alternative, even though they are still considerably slower than global mechanisms for multidimensional simulations.

On the subject of chemical reaction models, the use of flamelet-based techniques for the solution of multidimensional flames has been explored. The Flamelet Generated Manifold (FGM) method consists on the use of sets of flamelets for the construction of a manifold, a table, where thermochemical data can be stored and used for the solution of

higher dimension flames. This technique has proven to be orders of magnitude faster compared to multidimensional detailed chemistry solutions while still being highly accurate. The FGM method is based on the use of control variables to correctly map dependent quantities. In the case of premixed flames, enthalpy can be employed to reliably map heat loss. For non-premixed flames though, as enthalpy varies throughout the flame, it cannot be used in the same way. Instead, the enthalpy defect, a function of the enthalpy of the flame and of the mixture fraction, has been shown to be promising in this regard.

In this work the effect of radiative heat loss will be explored for non-premixed laminar methane / air flames near extinction, employing both detailed chemistry and the FGM method.

1.1 Literature Review

1.1.1 Radiation Modeling

As previously mentioned, thermal radiation, being one of the main processes for heat transfer in combustion, is also one of the most challenging aspects for the numerical treatment of reactive flows due to the strong coupling with chemical kinetics. Thermal radiation itself is calculated through the Radiative Transfer Equation (RTE), which has both a spatial dependency, usually solved with the use of the Discrete Ordinates Method (DOM), [Chandrasekhar, 1960] as well as a spectral dependency.

Several approaches to the spectral dependency have been proposed over time, some of the most common being the Grey Gas approach, the Weighted Sum of Grey Gases (WSGG) [Hottel and Sarofim, 1967], the Optically Thin Approximation (OTA) [Peters and Rogg, 1993], the Spectral Line-Based Weighted Sum of Gray Gases (SLW) [Denison and Webb, 1993], the Absorption-Line Blackbody Distribution Function (ALBDF) [Denison and Webb, 1993] and the the Cumulative Wavenumber model (CW) [Solovjov and Webb, 2002]. While relatively good results can be found with these models, the exact solution for the spectral component can be calculated by Line By Line integration (LBL) [Taine, 1983], though this is a very computationally demanding method. For the simplified models, WSGG in particular has been shown to be a good compromise between computational time and numerical accuracy [Mossi, 2011; Dorigon et al., 2013; Centeno et al., 2016, 2018]. These tools however, have been up to now commonly developed and

explored mainly in decoupled idealized one-dimensional and optically thick problems with imposed profiles for temperature and chemical species or use simplified chemical models. The ability to solve simultaneously both the detailed chemistry, reactive flow and the radiative heat loss in a coupled manner is important for a deeper understanding of the broad range of phenomena present in combustion, this being the subject of extensive study for the last decades [Taylor and Foster, 1974; Smith et al., 1982; Modest and Zhang, 2001; Maurente et al., 2008; Chu et al., 2011; Johansson et al., 2011; Centeno et al., 2014, 2016, 2018].

Overall, radiative heat loss plays a significant part on energy efficiency, safety and stability of the combustion process. For near extinction conditions, radiation has a major role in the maintenance of the flame. The OTA model was employed for the study of flammability limits in premixed methane flames by Ju et al., 1997. This work discussed how flame extinction occurs due to radiative heat loss, for low stretch rates, and due to low residence time for high stretch rates. It also presented how, at low equivalence ratios, flame stretch can improve flammability and enable combustion.

Liu et al., 2004, explored the effects of radiation for laminar methane/air diffusion flames. Coupled equations of radiation, flow and chemical kinetics were solved for a two-dimensional geometry. For the radiation treatment, a combination of the DOM/SNBCK method [Goutière et al., 2000] was compared to the simplified OTA model, with the inclusion of CO_2, H_2O, CO and soot. While re-absorption was shown to not have a major role for this configuration, the OTA model still underpredicts the flame's temperature by a small margin due to not taking reabsorption into account. Finally, a model with nine non-uniform bands was suggested for the calculation of non-gray radiation when soot is present.

The effect of radiation heat loss on the extinction of spherical premixed flames in microgravity were studied by Qiao et al., 2010, employing both experimental and numerical approaches. Methane/air flames were diluted with different gas compositions. Both an optically thick model, based on the Discrete Transfer Method [Liu, 1994], and OTA were used to determine burning velocity and compared to the experimental results, where the OTA model was shown to underpredict flame speed. Once more this is attributed to the lack of reabsorption. On the other hand, the optically thick method overpredicted these same results, in contrast to the experiment.

Mossi, 2011, studied the applicability of four radiation models: GG, WSGG, SLW and CW for the solution of a sooting laminar methane/air flame. The 2D adiabatic flame was solved first, with the decoupled radiation effects being added later. While the CW model presented unexpected convergence issues, only minor differences were found for the first three, with the caveat that the Grey Gas model should be used with caution and in specific conditions of optically thin limit or high soot formation. The author also showed that the WSGG model was 30% faster in relation to the spectral SLW model, proving to be a promising alternative for radiation treatment.

More recently, Centeno et al., 2016, studied the effect soot has on the raditive heat transfer for turbulent non-premixed methane-air flames, using both the superposition WSGG model and the Line-by-Line integration method with a global 2-step chemical mechanism. It was shown that the WSGG results were highly accurate compared to LBL, with normalized errors of 4.8 % and 1.2 % (maximum and average respectively) when soot is included, while requiring only 1/7000 of the LBL computational effort. In a subsequent study, Centeno et al., 2018, compared superposition and fixed uniform ratio WSGG models to the LBL solution for laminar ethylene flames, showing that for this case the uniform ratio model better approached the LBL solution. Once again it was shown that the inclusion of soot increased the WSGG model accuracy.

Specifically on the matter of diluted non-premixed reactive flows, the addition of CO_2 was numerically studied by Lee et al., 2001. One-dimensional counterflow flames were modeled with the use of the GRI 2.11 detailed mechanism and the optically thin radiation model based on CH_4, CO_2, CO and H_2O. The authors showed that the inclusion of carbon dioxide increases the effect of thermal radiation, making essentially important at low strain rates, where radiative heat loss dominates strain rate effects.

Furthermore, Bundy et al., 2003, studied methane-air flames diluted with N_2 and CO_2. Experiments were carried out on a counterflow burner, with the authors providing profiles for the extinction limits due to dilution for a wide range of strain rates. As expected, the extinction limits for the CO_2 dilution were considerably lower than for N_2, since carbon dioxide is both a chemically reacting and highly radiative emitting species. Hamins et al., 2007, used this same configuration to explore the extinction limits with nitrogen dilution for microgravity conditions, both experimentally and numerically. Both 1D and 2D simulations employed a three-step mechanism for the oxidation of methane

and an OTA model again based on CH_4, CO_2, CO and H_2O with no inclusion of soot. It was shown that one-dimensional flames could not faithfully reproduce experimental flames at low strain rates, especially for 1g conditions, due to the lack of lateral heat losses and buoyancy models. The authors also showed that the extinction process differs greatly for normal and microgravity conditions due to flame structure. These findings were later confirmed and expanded by Oh et al., 2008, using a similar setup to explore flame structure in finer detail. Once more, numerical flames were explored with the use of a three-step mechanism and the optically thin model.

Subsequently, Wang et al., 2013, studied the chemical and physical effects of CO_2 addition on methane/oxygen counterflow diffusion flames at a high strain rate. The authors employed a detailed mechanism with 197 species and 779 reactions to investigate the effects of different parameters on temperature and emission index of carbon monoxide (EICO). Overall, the authors pointed out that the addition of CO_2 helps to reduce flame's temperature due to its thermochemical effects while the addition of H_2O counterbalances this effect.

Finally, Mun et al., 2014, studied methane counterflow diffusion flames, diluted with both N_2 and CO_2, with the OTM and SNB models, showing that the latter generally better agrees to experimental data. This work unfortunately could only be found in Korean.

1.1.2 The FGM Method

In the past two decades, the Flamelet Generated Manifold (FGM) has proven to be a powerful tool for the numerical study of reactive flows. The technique was first presented by Van Oijen and de Goey, 2000, defined as a combination of two approaches: the use of flamelets, one-dimensional representations of a multi-dimensional flame, and the construction of a manifold, a low-dimensional data base where information from a set of flamelets can be stored and retrieved for subsequent calculations. Their study was directed at laminar premixed methane/air flames, employing one control variable, the progress variable. Starting with constant pressure, enthalpy and mass fractions, the FGM solution was compared to the ILDM method, developed by Maas and Pope, 1992, and the detailed solution. Simulations were compared for unit Lewis number, neglecting preferential diffusion. The authors described how to effectively manipulate boundary

conditions, temperature and composition, in order to achieve decreasing levels of enthalpy to correctly map the effects of heat loss on the premixed flame. The processes of storing and retrieving data from the manifold is also thoroughly described. The FGM solution proved to better describe the flame in relation to the ILDM method, especially for lower temperature regions, effectively matching the detailed solution, and at the same time, being orders of magnitude faster than the latter. The paper also suggested how the method could be expanded with additional control variables in order to calculate non-premixed flames.

Flame stretch was also studied by Van Oijen and de Goey, 2002, for premixed methane/air flames in the counterflow configuration, this would later prove to be an effective way of generating the sets of flamelets needed for the construction of a manifold.

Partially-premixed and non-premixed or diffusion flames have also been studied within the FGM technique. Fiorina et al., 2005, explored the usability of both the FPI (Flame Propagation of ILDM) [Gicquel et al., 2000] and FGM methods on laminar methane/air flames. The authors employed the mixture fraction Z as a second control variable, along with the progress variable, to correctly map the structure of the diffusion reactive flow for the counterflow configuration. These two control variables proved to be sufficient for handling the adiabatic diffusion flame. Ihme et al., 2012, further explored the optimization of the progress variable for methane/air mixtures, demonstrating that there was considerable room for improving the quality of flamelet- based models for either premixed, partially-premixed and non-premixed flames. A thorough review of the developments and employments of the FGM technique up to that point was presented in Van Oijen et al., 2016.

Hoerlle, 2015, utilized the FGM technique to study adiabatic laminar diffusion methane/air flames diluted with CO_2. Results were compared to a 4-step global mechanism showing that while the global mechanism represented well enough the overall flame characteristics, like temperature and H_2O formation, it showed small deviations when capturing CO_2 and fails to correctly represent other products formation, mainly CO and H_2, as well as not correctly describing local effects. The FGM however, accurately presented these local flame effects, such as flame stabilization, being at the same time orders of magnitude more efficient regarding computational time, even when accounting for the pre-processing phase (the actual construction of the manifold). The optimization of the

progress variable on both non-premixed methane and ethylene flames was also studied by Maders, 2018 with the use of a genetic algorithm. The authors found perfectly monotonic definitions of progress variable though the quality of the results for different definitions varied.

Although the modeling of heat loss in premixed and partially-premixed flames with the FGM technique has been well studied over the last decades there is scarcely any material on the simulation of heat loss for non-premixed or diffusion flames. The major issue being that, unlike premixed flames, the enthalpy on a diffusion flame is not constant along neither the spatial nor the composition axis, thus it is not a conserved scalar and cannot be directly used as a control variable to map heat loss. A clever approach to this problem is to employ a new variable, the enthalpy defect, which linearly depends on the enthalpy and can be shown to be constant along the entire flame's domain.

Even before the inception of the FGM method, Marracino and Lentini, 1997, proposed the use of the enthalpy defect to be used in place of the enthalpy for correctly representing and mapping radiative heat loss in the Stretched Laminar Flamelet (SLF) approach. In this method an adiabatic flame can be represented with the use of the scalar dissipation rate along with at least one conserved scalar, usually the mixture fraction. The enthalpy defect can be employed as the additional control variable for modeling non-adiabatic diffusion flames as long as the Lewis number is maintained at unity, an important limitation that ensures the defect levels are constant. With such, the work described the simulation of turbulent methane flames. The heat loss itself was modeled in terms of the enthalpy as a simple Stefan-Boltzmann model. Sets of flamelets with decreasing levels of enthalpy defects were assembled in a library, organized in what the authors described as "shelves", groups of flamelets which shared the same enthalpy defect, varying from 0 down to -700 kJ/kg in intervals of -50 kJ/kg. For each shelf the flamelets ranged from near equilibrium condition up to extinction. Intermediary values, not represented on any shelves, were calculated by linear interpolation. Overall the use of the enthalpy defect showed to considerably improve temperature and temperature pdf predictions over previous studies.

Hossain et al., 2001, employed the concept of enthalpy defect to simulate a bluff-body non-premixed flame. The authors described a method for achieving constant levels of enthalpy defect with the use of a counterflow configuration. This is ultimately the

same method used for this work and is thoroughly described in Chapter 4. The discrete transfer method was chosen for the modeling of the coupled radiation and the authors showed that however small the effects of heat loss were, it had a considerable influence on the prediction of OH levels. Once more though the work emphasizes how the use of unit Lewis number is required.

Further uses of enthalpy defect to treat heat loss continued to show up. Messig et al., 2013, performed an evaluation of different radiation modeling approaches for diffusion laminar flames. Unsteady flamelet solutions were employed for achieving a more detailed representation of the enthalpy defect, which resulted in variable values of enthalpy defect on the Z domain. The authors managed to attain accurate results for both unit and constant Lewis numbers, highlighting the importance of considering gas radiation for a more precise representation of flame structure. They also showed that for $Le = 1$, the use of unsteady flamelets produced very accurate solutions, while the steady constant enthalpy defects resulted in an overall lower temperature, with results improving with the use of more enthalpy defect intervals.

Recently, Breda et al., 2018 explored the use of the normalized enthalpy for simulating high pressure near-wall methane/oxygen flames on a 2D manifold. Simulations were realized for both laminar and turbulent regimes. For the laminar case it was shown that, on the fuel-rich side, the adiabatic flamelets better represented flame structure, while on the oxidant rich side the non-adiabatic flamelets yielded better results. A coupling of both approaches is suggested by the authors to correctly select either zone. Turbulent flames however presented underestimation of the wall heat flux. Temperature is finally suggested as an alternative control variable to handle heat loss, in place of enthalpy.

1.2 Objectives

The present work explores different thermal radiative solution methods for modeling laminar one-dimensional flames near the extinction condition, employing detailed chemistry and the Flamelet Generated Manifold chemistry reduction method.

The goals are divided as follow:

1. To generate flame solutions with coupled detailed chemistry, transport equations and radiation approaches.

2. To compare different thermal radiation solutions with literature data.

3. To implement the enthalpy defect as a control variable in the FGM method.

4. To solve and compare detailed and tabulated chemistry non-adiabatic flames.

1.3 Organization

Following the Introduction, Chapter 2 presents the basic formulation with fundamental equations to be followed for the rest of the Thesis. Chapter 3 explores the implementation and use of the WSGG model and LBL solution method in the one-dimensional flame code Chem1d. Chapter 4 introduces the use of the enthalpy defect as a control variable for the solution of non-premixed flames in the FGM technique in order to solve non-adiabatic diffusion flames. The final conclusions and discussion of future works are described in Chapter 5.

2 MATHEMATICAL MODEL FOR REACTIVE FLOWS

The conservation equations for reactive flows, along with its constitutive relations are presented in this chapter. These account for the conservation of total mass, mass of chemical species, momentum and energy. Also presented are the required thermodynamic relations, transport equations and equations of state. The formulation is based on laminar, non-premixed reactive flows at atmospheric conditions.

2.1 Conservation Equations

The Equation for the conservation of total mass (continuity equation) can be expressed in its general vector form as

$$\frac{\partial \rho}{\partial t} = -\nabla \cdot \ \rho\vec{u}, \tag{2.1}$$

where the left-handed side (LHS) represents the variation in time of the specific mass ρ, while $\vec{u}$ is the flow velocity. The conservation of mass can also be defined for a given chemical species i. The Equation in terms of its mass fraction Y_i reads

$$\frac{\partial(\rho Y_i)}{\partial t} + \nabla \cdot (\rho\vec{u}Y_i) = -\nabla \cdot \ \vec{V_i} + \dot{\omega}_i, \tag{2.2}$$

with $\vec{V_i}$ being the molecular diffusion velocity of species i in the mixture, while $\dot{\omega}_i$ represents the reaction source term. These quantities are described in the next subsection.

Next, the conservation of momentum, or the Navier-Stokes Equation(s) (NSE) is presented in its general form as

$$\frac{\partial(\rho\vec{u})}{\partial t} + \rho\vec{u} \cdot \nabla\vec{u} = -\nabla p + \nabla \cdot \tau + \rho\vec{g}. \tag{2.3}$$

Here, the terms on the LHS represents the local and convective accelerations. On the RHS are represented the normal (pressure) forces, shear (viscous) forces and body forces, with p being the static pressure, τ the stress tensor and $\vec{g}$ the gravity acceleration.

To complete the set of conservation equations, the conservation of energy can be written in terms of the the total specific enthalpy of the mixture, h. Considering constant pressure and neglecting viscous dissipation, the Equation reads

$$\frac{\partial(\rho h)}{\partial t} + \nabla \cdot (\rho \vec{u} h) = -\nabla \cdot \vec{q} + \dot{q}_R \tag{2.4}$$

with the term $\vec{q}$ being the heat flux vector and $\dot{q}_R$ being the source term for radiative heat losses.

2.2 Constitutive Relations and Approximations

Along with the above relations, the conservation equations are dependent on a number of defined quantities, namely the stress tensor τ, the velocity of mass diffusion $\vec{V}$, heat flux $\vec{q}$, reaction source term $\dot{\omega}_i$ and radiative source term $\dot{q}_R$. On this section, the equations for the first four terms are presented, while the modeling of the radiative source term is explored in Section 2.5.

The diffusion of linear momentum is accounted by the stress tensor τ, presented in Equation 2.3. Assuming Stokes hypothesis, the tensor can be written as

$$\tau = \mu[\nabla \vec{u} + (\nabla \vec{u})^T] - \frac{2}{3}\mu \nabla \cdot \vec{u} I, \tag{2.5}$$

with I being the identity tensor.

This work assumes steady flow at constant standard atmospheric pressure and room temperature (298 K), and since only laminar low-speed flames are modeled, a low Mach number approximation can be used. This results in very small pressure gradients and implies that these gradients have minimal effect over mass diffusion, being therefore negligible. The same can be applied for mass diffusion due to temperature gradients (Soret Effect), since it is only significant for very light species such as H_2 and He. Thus, mass diffusion is only carried out due to concentration gradients and can be modeled by Fick's Law:

$$\vec{V_i} = -\frac{D_i^M \nabla Y_i}{Y_i}, \tag{2.6}$$

with D_i^M being the coefficient of diffusion of species i in the mixture. The equation for the heat flux can be written in terms of the especific enthalpy as

$$\vec{q} = \frac{\lambda}{c_p}\nabla h + \sum_{i=1}^{N}\left(1 - \frac{1}{Le_i}\right)\frac{\lambda}{c_p} h_i \nabla Y_i \tag{2.7}$$

where the first term, in parenthesis, represents the heat conduction due to Fourier's

Law and the second term represents the heat diffusion due to mass diffusion. A term accounting for the second-order heat diffusion due to concentration gradients is omitted. This is known as the Dufour Effect and is usually neglected when modeling combustion processes [Coelho and Costa, 2007].

The reaction source term is derived from the mathematical modeling of detailed chemical kinetics. Considering the laminar reacting flow, a single forward reaction can be written as

$$\sum_{i=1}^{N} v_i' MW_i \overset{k_f}{\rightarrow} \sum_{i=1}^{N} v_i'' MW_i, \tag{2.8}$$

with k_f representing the forward reaction constant, and v_i' and v_i'' being the number of moles of species i for the reactant and product side. A complementary reverse reaction can be written as

$$\sum_{i=1}^{N} v_i'' MW_i \overset{k_r}{\rightarrow} \sum_{i=1}^{N} v_i' MW_i, \tag{2.9}$$

where k_r represents the reverse reaction constant. For a given generic elementary reaction such as

$$H_2 + O_2 \underset{k_r}{\overset{k_f}{\rightleftharpoons}} HO_2 + H, \tag{2.10}$$

following the Law of Mass Action, the forward reaction rate for the generation of product HO_2 is proportional to the concentration of reactants H_2 and O_2 by

$$\omega_{HO_2,f} = k_f [H_2][O_2], \tag{2.11}$$

with the reaction constant k_f given by the Arrhenius model:

$$k_f = A_r T^{\beta r} exp\left(-\frac{E_a}{R_u T}\right), \tag{2.12}$$

where A_r represents the pre-exponential factor, βr the dimensionless temperature exponent and E_a the activation energy in kJ.

Considering both directions for a given reaction with N species, the net reaction rate is then given by

$$\hat{\omega}_i = \hat{\omega}_{i,f} + \hat{\omega}_{i,b} = (v_i'' - v_i')\omega, \tag{2.13}$$

with the reaction rate ω written in terms of the concentration C as

$$\omega = k_f \prod_{i=1}^{N} C_i^{v_i'} - k_b \prod_{i=1}^{N} C_i^{v_i''}. \tag{2.14}$$

Since for the equilibrium state $\omega \equiv 0$, only one of the reaction rates has to be solved, as they both balance out and relate to the equilibrium constant $K_{c,j} = k_{f,j}/k_{r,j}$ for each reaction j, therefore the reaction rate ω can be written as

$$\omega = k_f \left(\prod_{i=1}^{N} C_i^{v_i'} - K_c^{-1} \prod_{i=1}^{N} C_i^{v_i''} \right). \tag{2.15}$$

Finally, the reaction source term, present in Equation 2.2 for all present elementary reactions N_r can be written as

$$\dot{\omega}_i = MW_i \sum_{j=1}^{N_r} \left(v_{i,j}'' - v_{i,j}' \right) \omega_j. \tag{2.16}$$

2.3 Auxiliary Relations

To close out the set of conservation equations a number of auxiliary relations are needed. A mixture-average transport model is employed, starting with the auxiliary equations and considering the ideal gas model, the specific mass of the mixture can be written as

$$\rho = \frac{p_0 MW}{R_u T}, \tag{2.17}$$

with MW representing the molecular weight for the mixture, $R_u = 8.314\ kJ/kmolK$ being the universal gas constant, T the temperature and p_0 the atmospheric pressure. This equation is carried out for the low Mach Number limit, where it can be assumed that $p \equiv p_0$.

Temperature is related to enthalpy by the calorific Equation of state

$$\Delta h = c_p \Delta T, \tag{2.18}$$

with c_p being the specific heat at constant pressure for the mixture. This can be calculated

by the equation

$$c_p = \sum_{i=1}^{N_s} c_{p,i} Y_i, \tag{2.19}$$

where $c_{p,i}$ is the specific heat at constant pressure for a given species, usually derived from polynomial empirical correlations.

The specific enthalpy of the mixture can be written as the sum of the enthalpies of all participating species

$$h = \sum_{i=1}^{N_s} Y_i h_i, \tag{2.20}$$

$$h_i = h_{i,f}^0 + \sum_{Tref}^{T} c_{p,i}(T) dT, \tag{2.21}$$

where $h_{i,f}^0$ is the specific enthalpy of formation for species i at a reference temperature T_{ref}.

The average mass diffusion coefficient D_i^M for a given species i in mixture m is calculated using the Hirschfelder and Curtiss approximation [Hirschfelder et al., 1954]:

$$D_i^M = \frac{1 - Y_i}{\sum_{i=1, i \neq j}^{N_s} X_j / D_{i,j}} \tag{2.22}$$

with $D_{i,j}$ taken from Turns, 2000, and X_j being the molar fraction for species j.

On the other hand. the mixture-average thermal conductivity λ is calculated by the semi-empirical formula of Mathur and Saxena, 1967

$$\lambda = \frac{1}{2} \left(\sum_{i=1}^{N} X_i \lambda_i + \left(\sum_{i=1}^{N} \frac{X_i}{\lambda_i} \right)^{-1} \right), \tag{2.23}$$

with λ_i being the thermal conductivity for a given species i. The thermal or heat diffusion can be written as

$$\alpha = \frac{\lambda}{\rho c_p}, \tag{2.24}$$

with c_p and ρ taken from Equation 2.19 and 2.17 respectively.

The dynamic viscosity can be calculated using the approximate expressions of Wilke, 1950:

$$\mu = \sum_{i=1}^{N_s} \frac{\mu_i}{1 + X_i^{-1} \sum_{j=1, j\neq i}^{N_s} X_j \phi_{i,j}}, \tag{2.25}$$

being that

$$\phi_{i,j} = \frac{1}{\sqrt{8}} \left(1 + \frac{MW_i}{MW_j}\right)^{-1/2} \left[1 + \left(\frac{\mu_i}{\mu_j}\right)^{1/2} \left(\frac{MW_j}{MW_i}\right)^{1/4}\right]^2. \tag{2.26}$$

The ratio between thermal and mass diffusivities is described by the Lewis number Le. Which for a single species i, can be written as

$$Le_i = \frac{\alpha}{D_i^M}. \tag{2.27}$$

Finally, a simplification of the transport model can be achieved with the use of a constant Lewis number, resulting in faster computational times. With such, following Smooke and Giovangigli, 1991, both the dynamic viscosity μ and the thermal conductivity λ can be approximated by temperature based functions of the form:

$$\frac{\mu}{c_p} = 1.67 \left(\frac{T}{298}\right)^{0.51}, \tag{2.28}$$

$$\frac{\lambda}{c_p} = 2.58 \left(\frac{T}{298}\right)^{0.69}. \tag{2.29}$$

For Chapter 3, mixture average properties will be assumed, while in Chapter 4, it is assumed that $Le_i = 1$ to avoid accounting for preferential diffusion and to ensure constant levels of enthalpy defect.

2.4 Final Forms of the Conservation Equations

The conservation equations can now be re-written considering the previously stated assumptions (laminar, low-speed flow at constant atmospheric pressure and room temperature).

Due to low speed (low Mach Number approximation), the specific mass of the mixture can be considered a function of the temperature only, which automatically simplifies Equation 2.1. Due to the use of a mixture-average approach, the conservation of mass for each species (Equation 2.2) does not amount to zero. This can be achieved though by solving this equation for $N - 1$ species, ensuring conservation. The Energy Equation

already assumed small pressure gradients, with both the pressure derivative and the viscous dissipation being negligible. With all of these considerations, the set of conservation Equations (2.1 - 2.4) can finally be simplified to the following forms:

$$\frac{\partial \rho}{\partial t} + \nabla \cdot \rho \vec{u} = 0, \tag{2.30}$$

$$\frac{\partial (\rho Y_i)}{\partial t} + \nabla \cdot (\rho \vec{u} Y_i) = \nabla \cdot (\rho D_i^M \nabla Y_i) + \dot{\omega}_i \qquad i = 1, ..., N-1, \tag{2.31}$$

$$\frac{\partial (\rho \vec{u})}{\partial t} + \rho \vec{u} \cdot \nabla \vec{u} = -\nabla p + \nabla \cdot \tau + \rho \vec{g}. \tag{2.32}$$

$$\frac{\partial (\rho h)}{\partial t} + \nabla \cdot (\rho \vec{u} h) = \nabla \cdot \left(\frac{\lambda}{c_p} \nabla h \right) - \nabla \cdot \left[\sum_{i=1}^{N} \left(1 - \frac{1}{Le_i} \right) \frac{\lambda}{c_p} h_i \nabla Y_i \right] + \dot{q}_R \tag{2.33}$$

2.5 Thermal Radiation Modeling

The solution for the radiative source term $\dot{q}_R$, presented in the Energy Equation (2.33), is the final goal of the thermal radiation modeling. This term represents the volumetric heat loss due to radiation, and is defined as the negative of the divergent of the radiative heat flux. Several approaches can be employed to obtain this quantity, each approach with its particular degree of detail, accuracy and complexity. Also, although it is known that the inclusion of soot dramatically increasin radiative emissions, the amount of soot generated for highly diluted methane / air flames is minimal and its effects can be neglected.

2.5.1 Optically Thin Approximation

Possibly, the simplest available radiation model employed in combustion is the approximation for an optically thin medium (Optically Thin Approximation - OTA). This method considers the Grey Gas (GG) hypothesis for the spectral model, in which the absorption coefficient does not depend on the wave number, and at the optically

thin limit, absorption is neglected, considering that only emission is responsible for the radiative heat transfer. Thus, the Radiative Transfer Equation (RTE) does not need to be solved. Due to this simplification, the OTA model is computationally very fast, and while not as precise as RTE-solving approaches, it can still improve results significantly when compared to the adiabatic solution.

The radiation source term is given by

$$\dot{q}_R = -4\sigma k_p (T^4 - T_\infty^4), \tag{2.34}$$

where T_∞ is the room temperature and σ is the Stefan-Boltzmann constant. The term k_p is the mean Planck absorption coefficient for the grey-medium, obtained from

$$k_p = \sum_{i=1}^{N_{gg}} p_i k_{p,i}, \tag{2.35}$$

being that N_{gg} is the number of grey-gases, p_i the partial pressure and $k_{p,i}$ the Planck absorption coefficient for each gas i. The actual number of grey-gases employed can vary. This work investigated both the solution for two gases (CO_2 and H_2O) as well as the more common four gases consideration (H_2O, CO_2, CH_4 and CO). The absorption coefficients are taken from Peters and Rogg, 2993, for CO_2 and H_2O, and from Sandia National Laboratories [Sandia, 2016] for CH_4 and CO.

2.5.2 Radiative Transfer Equation

A more precise method for calculating the radiative source term is the solution of the Radiative Transfer Equation (RTE), which describes the radiative intensities for an emitting and absorbing participating medium. The spectral form of the RTE is solved for the entire thermal radiative spectrum and for a given number of angular directions.

For each S direction in a non-scattering medium, the RTE is written as

$$\frac{\partial I_\eta}{\partial S} = -\kappa_\eta(S) I_\eta(S) + \kappa_\eta(S) I_{\eta,b}(S, \Omega_l), \tag{2.36}$$

where κ_η is the spectral absorption coefficient, I_η accounts for the reduction of intensity due to reabsorption, $I_{\eta,b}$ represents the increase in intensity due to black body emission and Ω_l is the solid angle.

The angular dependency can be calculated by the Discrete Ordinate Method

(DOM), proposed by Chandrasekhar, 1960. This method describes the radiative intensity along a direction S in a discrete form of the total solid angle of 4π. Regarding the 1D case, in DOM, the spectral intensities are solved for each hemisphere of the solid angle, resulting in equations for the positive ($I^+(S)$) and negative intensity ($I^-(S)$) directions. Figure 2.1 illustrates the directions of the solid angle. An angular discretization of fifteen is considered in each hemisphere of the total solid angle for this thesis, as no significant increase in quality was found with more directions.

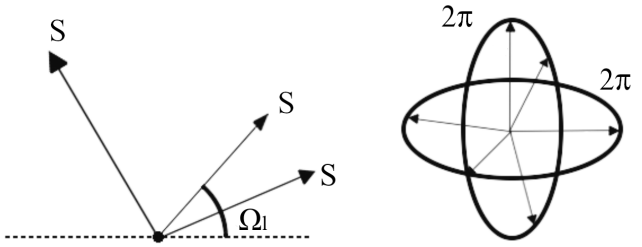

Figure 2.1 – Representation of the solid angle 4π.

At the same time, the spectral dependency of the RTE is solved by either the Line-By-Line (LBL) integration method or the Weighted Sum of Grey-Gases (WSGG) model. For this work, both approaches consider a participating medium composed only of CO_2 and H_2O.

2.5.3 Line-By-Line Integration

The Line-By-Line integration method (LBL), determines the absorption coefficient of the participating species for the whole spectrum. This represents the exact solution of the spectral dependency for the radiative problem.

The method is based on the discretization of the HITEMP 2010 Spectral Properties Database [Rothman et al., 2010], in terms of wave-number, to determine the participating gases radiative properties. This work employed 30000 lines generated for a wave-number (η) interval ranging from 10^4 cm^{-1} to 10^{-4} cm^{-1}, which is usually the spectrum range of interest for radiation heat transfer [Ziemniczak, 2014], and for temperatures ranging from 296 K to 2500 K. As HITEMP database does not provide spectral properties for temperatures below 1000 K, the extrapolated values from Ziemniczak, 2014 were used. A complete description of the database generation is found in Dorigon et al., 2013, Cassol

et al., 2014.

The spectral absorption coefficient per unit pressure is given by

$$\kappa_{\eta,p} = \frac{\kappa_\eta}{p}, \tag{2.37}$$

being p is the partial pressure of the participating media. For simplicity, the notation $\kappa_{\eta,p} = \kappa_\eta$ is used. The black-body radiation intensity is computed from the Planck's distribution. Finally, the volumetric heat generation is obtained from the divergent of the radiative heat flux [Ziemniczak, 2014] and is written as

$$\dot{q}_R(S) = \sum_{l=1}^{15} \sum_{\eta=1}^{30000} [2\pi\kappa_\eta \Omega_l [I^+_{\eta,l}(S) + I^-_{\eta,l}(S)] - 4\pi\kappa_\eta I_{\eta,b}]. \tag{2.38}$$

2.5.4 Weighted Sum of Grey Gases

While the LBL method results in the exact solution for the radiative problem, it is also computationally demanding when compared to models like OTA, and serves primarily as a benchmark solution. If it is possible to assume that a portion $\Delta\eta$ of the radiative spectrum can be represented by a given a grey-gas i, and that each pressure absorption coefficient κ_i does not depend on temperature, but only on the partial pressure of the participating species, the WSGG model [Hottel and Sarofim, 1967] can be used as an alternative.

In this approach, the absorption coefficient dependence on the wave-number is decoupled from the thermodynamical state, thus, the RTE for an emitting, absorbing non-scattering medium becomes

$$\frac{\partial I}{\partial S} = \kappa_i \left(a_i \frac{\sigma T^4(s)}{\pi} - I_i(S) \right), \tag{2.39}$$

where the first term on the RHS represents the black-body intensity and $I_i(S)$ is the radiative intensity for the grey-gas i.

The term a_i represents the temperature dependent weighting coefficient for the i-th grey gas, which can be written as

$$a_i(T) = \sum_{j=0}^{J} b_{i,j} T(S)^j, \tag{2.40}$$

where $b_{i,j}$ indicates the polynomial coefficients of j order from the gas i.

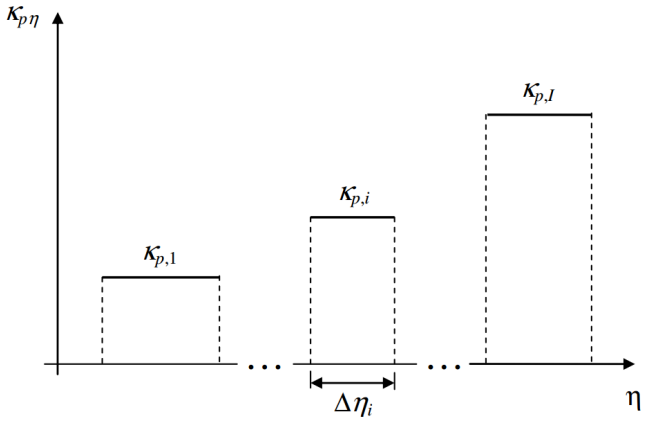

Figure 2.2 – Representation of absorption coefficients in the WSGG model for I grey-gases [Dorigon et al., 2013].

For the present work, the WSGG model depends on the specific pressure absorption coefficients for each participating species, which consists of combinations of H_2O and CO_2, plus a transparent window, a region where the absorption coefficient can be considered zero. Different values of κ_p can be used for different species and ratios. This thesis employs a fixed 1:1 as well as a 2:1 H_2O/CO_2 ratio, both of which are presented in Tables 2.1 and 2.2 respectively. It is to be assumed that the ratio of 2:1 is employed in all following simulations, unless stated otherwise.

Table 2.1 – Polynomial Absorption Coefficients for WSGG Model for a ratio of $p_{H_2O}/p_{CO_2} = 1$ [Ziemniczak, 2014].

n	$\kappa_i(atm\ m) - 1$	$b_{i,1}$	$b_{i,2}(K^{-1})$	$b_{i,3}(K^{-2})$	$b_{i,4}(K^{-3})$	$b_{i,5}(K^{-4})$
1	1.75E-01	6.12E-02	8.83E-04	-9.79E-07	4.68E-10	-7.93E-14
2	1.48E+00	1.03E-01	3.53E-04	-2.78E-07	6.71E-11	-4.86E-15
3	9.62E+00	2.19E-01	-1.05E-04	3.22E-08	-1.55E-11	3.15E-15
4	1.25E+02	8.74E-02	5.53E-05	-1.24E-07	5.41E-11	-7.33E-15

Table 2.2 – Polynomial Absorption Coefficients for WSGG Model for a ratio of $p_{H_2O}/p_{CO_2} = 2$ [Ziemniczak, 2014].

n	$\kappa_i(atm\ m) - 1$	$b_{i,1}$	$b_{i,2}(K^{-1})$	$b_{i,3}(K^{-2})$	$b_{i,4}(K^{-3})$	$b_{i,5}(K^{-4})$
1	0.1803	5.0431E-02	7.8873E-04	-8.5656E-07	4.2041E-10	-7.3022E-14
2	1.5144	1.1508E-01	2.5808E-04	-1.1058E-07	-2.0181E-11	9.5956E-15
3	9.40755	1.7626E-01	1.2709E-04	-2.2646E-07	9.5142E-11	-1.3444E-14
4	101.5430	1.2522E-01	-1.2309E-05	-8.3104E-08	4.3438E-11	-6.3142E-15

The conservation of radiative energy is ensured by the fraction of the black-body emission associated with the transparent window, which is defined as $a_0(T) = 1 - \sum_{j=0}^{J} a_i(T)$, with the polynomial coefficients obtained from Ziemniczak, 2014.

Finally, the thermal radiation heat source for the WSGG model can be written as

$$\dot{q_R}(S) = \sum_{i=1}^{4}\sum_{l=1}^{15} 2\pi\Omega_l k_{p,i} p_a(S)[[I_{i,l}^{+}(S) - I_{i,l}^{-}(S)] - 2a_i(S)I_b(S)]. \tag{2.41}$$

2.6 Flamelet Formulation

The simulation of multi-dimensional reactive flows is a very computationally demanding process. It is possible, however, to consider a multi-dimensional flame as a collection of one-dimensional flame structures called flamelets. A set of conservation equations for the solution of the flamelets was developed by de Goey and Boonkkamp, 1999. These represents the solution for the transport equations of the flame and detailed chemical kinetic processes, decoupled from the flow equations.

Beginning with the conservation of total mass, it reads

$$\frac{\partial \rho u}{\partial x} = -\rho K, \tag{2.42}$$

which is similar to the previously presented equations for a single dimension, except for the inclusion of the strain rate K, a quantity that accounts for the multi-dimensional effects not present in one-dimensional analysis.

Similarly, the mass conservation for a chemical species i is defined in terms of its

mass fraction as

$$\frac{\partial(\rho u Y_i)}{\partial x} = \frac{\partial}{\partial x}\left(\rho D_i^M \frac{\partial Y_i}{\partial x}\right) + \dot{\omega}_i - \rho K Y_i, \tag{2.43}$$

with the multi-dimensional gradients being replaced by a single partial derivative in the x direction.

The energy conservation equation reads

$$\frac{\partial(\rho u h)}{\partial x} = \frac{\partial}{\partial x}\left(\frac{\lambda}{cp}\frac{\partial h}{\partial x} + \sum_{i=1}^{N} \rho D_i^M h_i \frac{\partial Y_i}{\partial x}\right) - \rho K h + \dot{q}_R. \tag{2.44}$$

An equation for the conservation of the stretch is written as

$$\frac{\partial \rho u K}{\partial x} = \frac{\partial}{\partial x}\left(\mu \frac{\partial K}{\partial x}\right) - \rho K^2 + (\rho a^2)_{ox}, \tag{2.45}$$

being that the subscript ox accounts for the oxidant side. The term a represents the strain rate at the oxidant side, and is written as

$$a = -\frac{\partial u}{\partial x}, \tag{2.46}$$

which can be understood simply as the velocity gradient of the flow.

REFERENCES

Bilger, R. W. The Structure of turbulent nonpremixed flames, **Symposium (International) on Combustion**, vol. 22(1), p. 475–488, 1989.

Breda, P., Zips, J., and Pfitzner, M. **A Non-Adiabatic Flamelet Approach for Non-Premixed O2-CH4 Combustion**. In Proceedings of the 3rd World Congress on Momentum, Heat and Mass Transfer, Budapest, Hungary, 2018.

Bundy, M., Hamins, A., and Lee, K. Y. Suppression limits of low strain rate non-premixed methane flames, **Combustion and Flame**, vol. 133, p. 229 – 310, 2003.

Cassol, F., Brittes, R., Centeno, F., Silva, C., and França, F. Evaluation of the gray gas model to compute radiative transfer in non-isothermal, non-homogeneous participating medium containing CO 2 , H 2 O and soot, **The Brazilian Society of Mechanical Sciences and Engineering**, 2014.

Centeno, F. R., Brittes, R., França, F. H., and da Silva, C. V. Application of the WSGG model for the calculation of gas–soot radiation in a turbulent non-premixed methane–air flame inside a cylindrical combustion chamber, **International Journal of Heat and Mass Transfer**, vol. 93, p. 742–753, 2016.

Centeno, F. R., Brittes, R., Rodrigues, L. G., Coelho, F. R., and França, F. H. Evaluation of the WSGG model against line-by-line calculation of thermal radiation in a non-gray sooting medium representing an axisymmetric laminar jet flame, **International Journal of Heat and Mass Transfer**, vol. 124, p. 475–483, 2018.

Centeno, F. R., Silva, C. V., and França, F. H. R. The influence of gas radiation on the thermal behavior of a 2D axisymmetric turbulent non-premixed methane–air flame, **Energy Conversion and Management**, vol. 79, p. 405–414, 2014.

Chandrasekhar, S. **Radiative Transfer**. Dover Publications, 1960.

Chelliah, H., Law, C., Ueda, T., Smooke, M., and Williams, F. **Proceedings of Combustion Institute**, vol. 23, p. 503 – 511, 1990.

Chu, H., Liu, F., and Zhou, H. Calculations of gas thermal radiation transfer in one-dimensional planar enclosure using LBL and SNB models, **International Journal of Heat and Mass Transfer**, vol. 54(21-22), p. 4736–4745, 2011.

Claerbout, J. F., **Fundamentals of Geophysical Data Processing**, vol. Fundamentals of Geophysical Data Processing, chapter Sylvester's Matrix Theorem. Stanford University, fundamentals of geophysical data processing edition, 1976.

Coelho, P. and Costa, M. **Combustão**. Orion, 2007.

de Goey, L. P. H. and Boonkkamp, J. H. M. T. A flamelet description of premixed laminar flames and the relation with flame stretch, **Combustion and Flame**, vol. 119(3), p. 253–271, 1999.

Denison, M. and Webb, B. An absorption-line blackbody distribution function for efficient calculation of total gas radiative transfer, **Journal of Quantitative Spectroscopy and Radiative Transfer**, vol. 50(5), p. 499–510, 1993.

Dorigon, L. J., Duciak, G., Brittes, R., Cassol, F., Galarça, M., and França, F. WSGG correlations based on HITEMP2010 for computation of thermal radiation in non-isothermal, non-homogeneous H2O/ CO2 mixtures, **International Journal of Heat and Mass Transfer**, vol. 64, p. 863 – 873, 2013.

EIA. **Annual Energy Outlook 2020**. techreport, U.S. Energy Information Administration, 2020.

Fiorina, B., Gicquel, O., Vervisch, L., Carpentier, S., and Darabiha, N. Approximating the chemical structure of partially premixed and diffusion counterflow flames using FPI flamelet tabulation, **Combustion and Flame**, vol. 140, p. 147–160, 2005.

Gicquel, O., Darabiha, N., and Venin, D. T. Laminar Premixed Hydrogen/air Counterflow Flame Simulations Using Flame Prolongation of ILDM with Differential Diffusion, **Proceedings of the Combustion Institute**, vol. 28, p. 1901–1908, 2000.

Goutière, V., Liu, F., Charette, A., and Quant, J. An assessment of real-gas modelling in 2D enclosures, **Spectrosc. Radiat. Transfer**, vol. 64, p. 299 – 326, 2000.

Hamins, A., Bundy, M., Oh, C., and Kim, S. Effect of buoyancy on the radiative extinction limit of low-strain-rate nonpremixed methane–air flames, **Combustion and Flame**, vol. 151(225 - 234), 2007.

Hirschfelder, J., Curtiss, C., and Bird, R. **Molecular theory of gases and liquids**. Wiley New York, 1954.

Hoerlle, C. **Estudo Numérico de Chamas Laminares Difusivas de CH4 Diluído com CO2 Empregando Mecanismos Cinéticos Globais e a Técnica Flamelet-Generated Manifold**. Master's thesis, Universidade Federal do Rio Grande do Sul, Porto Alegre, Brasil, 2016.

Hossain, M., Jones, J. C., and Malalasekera, W. Modelling of a Bluff-Body Nonpremixed Flame Using a Coupled Radiation/Flamelet Combustion Model, **Flow, Turbulence and Combustion**, vol. 67, p. 217–234, 2001.

Hottel, H. and Sarofim, A. **Radiative Tranfer**. McGraw-Hill, New York, 1967.

IEA. **Key World Energy Statistics**. techreport, International Energy Agency, 2019.

Ihme, M., Shunn, L., and Zhang, J. Regularization of reaction progress variable for application to flamelet-based combustion models, **Combustion and Flame**, vol. 231, p. 7715–7721, 2012.

Johansson, R., Leckner, B., Andersson, K., and Johnsson, F. Account for variations in the H2O to CO2 molar ratio when modelling gaseous radiative heat transfer with the weighted-sum-of-grey-gases model, **Combustion and Flame**, vol. 158(5), p. 893–901, 2011.

Ju, Y., Guo, H., Maruta, K., and Liu, F. On the extinction limit and flammability limit of non-adiabatic stretched methane–air premixed flames, **Journal of Fluid Mechanics**, vol. 342, p. 315 – 334, 1997.

Law, C. **Combustion Physics**. Cambridge University Press, 2010.

Lee, C., Lee, S., Han, J., and Park, J. Numerical study on the effect of CO2 addition in flame structure and NOx formation of CH4-air counterflow diffusion flames, **International Journal of Energy Research**, vol. 25, p. 343 – 354, 2001.

Liu, F., Guo, H., and Smallwood, G. Effects of radiation model on the modeling of a laminar coflow methane/air diffusion flame, **Combustion and Flame**, vol. 138, p. 136 – 154, 2004.

Liu, Y. **PhD thesis**. PhD thesis, Department of Engineering, University of Cambridge, 1994.

Lutz, A. E., Kee, R. J., Grcar, J. F., and Rupley, F. M. **OPPDIF: A Fortran program for computing opposed-flow diffusion flames**. Technical report, Sandia National Labs, 1997.

Maas, A. and Pope, S. B. Simplifying Chemical Kinetics: Intrinsic Low-Dimensional Manifolds in Composition Space, **Combustion and Flame**, vol. 88, p. 239–264, 1992.

Maders, L. **Study of Progress Variable Definition of Flamelet-Based Models Using Optimization Algorithm**. Master's thesis, Universidade Federal do Rio Grande do Sul, Porto Alegre, Brasil, 2018.

Marracino, B. and Lentini, D. Radiation Modelling in Non-Luminous Nonpremixed Turbulent Flames, **Combustion Science and Technology**, vol. 128(1-6), p. 23–48, 1997.

Maruta, K., Yoshida, M., Guo, H., Ju, Y., and Niioka, T. Extinction of Low-Stretched Diffusion Flame in Microgravity, **Combustion and Flame**, vol. 112, p. 181 – 186, 1998.

Mathur, S. and Saxena, S. C. Methods of calculating thermal conductivity of binary mixtures involving polyatomic gases, **Applied Scientific Research**, 1967.

Maurente, A., Vielmo, H., and França, F. Comparison of the standard weighted-sum-of-gray-gases with the absorption-line blackbody distribution function for the computation of radiative heat transfer in H2O/ CO2 mixtures, **Journal of Quantitative Spectroscopy & Radiative Transfer**, vol. 109, p. 1758 – 1770, 2008.

Messig, D., Hunger, F., Keller, J., and Hasse, C. Evaluation of radiation modeling approaches for non-premixed flamelets considering a laminar methane air flame, **Combustion and Flame**, vol. 160, p. 251–264, 2013.

Modest, M. F. and Zhang, H. The Full-Spectrum Correlated-k Distribution for Thermal Radiation From Molecular Gas-Particulate Mixtures, **Journal of Heat Transfer**, vol. 124(1), p. 30–38, 2001.

Mossi, A. **Modelagem da radiação térmica em chamas laminares da combustão de metano em ar**. PhD thesis, Universidade Federal do Rio Grande do Sul, 2011.

Mun, S., Cho, J., Hwang, C., Oh, C. B., and Park, W. Effect of Radiation Models on the Suppression Limits in Counterflow Methane/Air Diffusion Flames, **Fire Sci. Eng., Vol. 28, No. 3, pp. 20-28, 2014**, 2014.

Oh, C., Hamins, A., Bundy, M., and Park, J. The two-dimensional structure of low strain rate counterflow nonpremixed-methane flames in normal and microgravity, **Combustion Theory and Modelling**, vol. 12.2, p. 283 – 302, 2008.

Peters, N. and Rogg, B. Reduced kinetic mechanisms for applications in combustion systems, **Lecture Notes in Physics**, vol. 15, 1993.

Poinsot, T. and Veynante, D. **Theoretical and Numerical Combustion - Second Edition**. Edwards, 2001.

Qiao, L., Gan, Y., Nishiie, T., Dahm, W., and Oran, E. Extinction of premixed methane/air flames in microgravity by diluents: Effects of radiation and Lewis number, **Combustion and Flame**, vol. 157, p. 1446 – 1455, 2010.

Rothman, L., Gordon, I., Barber, R., Dothe, H., R.R., G., Goldman, A., Perevalov, V., Tashkun, S., and Tennyson, J. HITEMP, the high-temperature molecular spectroscopic database, **Journal of Quantitative Spectroscopy & Radiative Transfer**, vol. 111, p. 2139 – 2150, 2010.

Sandia. **International Workshop on Measurement and Computation of Turbulent Nonpremixed Flames (TNF)**, 2016.

Smith, T. F., Shen, Z. F., and Friedman, J. N. Evaluation of Coefficients for the Weighted Sum of Gray Gases Model, **Journal of Heat Transfer**, vol. 104(4), p. 602–608, 1982.

Smooke, M. D. and Giovangigli, V. Formulation of the Premixed and Nonpremixed Test Problems, **Lecture Notes in Physics**, vol. 384, 1991.

Solovjov, V. P. and Webb, B. W. A local-spectrum correlated model for radiative transfer in non-uniform gas media, **Journal of Quantitative Spectroscopy and Radiative Transfer**, vol. 73(2-5), p. 361–373, 2002.

Somers, B. **The simulation of flat flames with detailed and reduced chemical models**. Eindhoven University of Technology, 1994.

Taine, J. A line-by-line calculation of low-resolution radiative properties of CO2-COtransparent nonisothermal gases mixtures up to 3000K, **Journal of Quantitative Spectroscopy & Radiative Transfer**, vol. 30-4, p. 371 – 379, 1983.

Taylor, P. and Foster, P. The total emissivities of luminous and non-luminous flames, **International Journal of Heat and Mass Transfer**, vol. 17(12), p. 1591–1605, 1974.

Turns, S. R. **An Introduction to Combustion**. McGraw Hill, 2nd edition, 2000.

Van Oijen, J. A., A Donini, R. J. M. B., ten Thije Boonkkamp, J. H. M., and de Goey, L. P. H. State-of-the-art in premixed combustion modeling using flamelet generated manifolds, **Progress in Energy and Combustion Science**, vol. 57, p. 30–74, 2016.

Van Oijen, J. A. and de Goey, L. P. H. Modelling of Premixed Laminar Flames using Flamelet-Generated Manifolds, Combustion Science and Technology, **Combustion Science and Technology**, vol. 161(1), p. 113–137, 2000.

Van Oijen, J. A. and de Goey, L. P. H. Modelling of Premixed Counterflow Flames Using the Flamelet-Generated Manifold Method, **Combustion Theory Modelling**, vol. 6, p. 463–478, 2002.

Wang, L., Liu, Z., Chen, S., C., Z., and Li, J. Physical and Chemical Effects of CO2 and H2O Additives on Counterflow Diffusion Flame Burning Methane, **Energy Fuels**, vol. 27, p. 7602 – 7611, 2013.

Wilke, C. R. A viscosity equation for gas mixtures, **Combustion and Flame**, vol. 18(4), p. 517–517, 1950.

Ziemniczak, A. **Geração de novas correlações da soma-ponderada-de-gases-cinza para espécies individuais de gases participantes: H2O, CO2, CO e CH4**. Master's thesis, Universidade Federal do Rio Grande do Sul, 2014.